



Elucidation of keyhole induced bubble formation mechanism in fiber laser welding of low carbon steel

Dongsheng Wu, Xueming Hua*, Lijin Huang, Fang Li, Yan Cai

Shanghai Key Laboratory of Material Laser Processing and Modification (Shanghai Jiaotong University), Shanghai 200240, PR China
Collaborative Innovation Center for Advanced Ship and Deep-Sea Exploration, Shanghai 200240, PR China

ARTICLE INFO

Article history:

Received 23 January 2018

Received in revised form 19 July 2018

Accepted 21 July 2018

Keywords:

Laser welding

Keyhole behavior

Multi-reflection

Keyhole-induced porosity

Keyhole-induced bubble

ABSTRACT

Laser welding experiment with the aid of glass, and numerical simulation are carried out to study the keyhole behavior and keyhole-induced bubble formation. Two mechanisms are responsible for keyhole-induced bubble formation. The first mechanism is the strong fluid flow inside the weld pool, and the capillary instability of the whole keyhole, causing the collapse between rear keyhole wall and front keyhole wall. This mechanism contributes to most of keyhole-induced bubble formation. The second mechanism is the instability of the rear keyhole wall caused by the increase absorption of laser energy reflected by the bulge at front keyhole wall. The breaking of molten bridge is analyzed based on static pressure balance. The molten bridge with large curvature and low temperature is difficult to be broken. Bubble coalescence can be clearly observed at the bottom of the weld pool. Large bubble and small bubble have high coalescence efficiency. The bubbles at keyhole bottom have more time to escape without broken by laser beam, and the bottom part of rear keyhole wall is more easily depressed, so bubbles are easily formed at the keyhole bottom.

© 2018 Elsevier Ltd. All rights reserved.

1. Introduction

Keyhole-induced porosity is a general defect in laser welding [1]. During laser welding, the keyhole is unstable, which causes the formation of keyhole-induced bubble. When the bubble is trapped by the solidified front in the rear part of the weld pool, keyhole-induced porosity is formed [2]. In order to suppress the keyhole-induced porosity formation and improve the weld quality, some effective measures had been proposed, such as using a side gas jet [3], forward welding [4], vacuum welding [5], N₂ shielding gas [6], applying electromagnetic force [7], laser power modulation [8], tandem laser welding [9].

The high speed X-ray transmission system was used to observe the keyhole behavior in laser welding, and gave a deep insight on the bubble formation mechanism. Katayama [10] and Matsunawa [11] proposed that the keyhole rear wall instability and depression caused by localized evaporation of the front keyhole wall led to the bubble formation. Seto [12] suggested that due to the extremely vigorous expansion and contraction of the keyhole, bubbles were intermittently formed at the keyhole tip. Heider [13] showed that due to keyhole bending, the absorption of laser energy at the

keyhole tip was increased, which caused the strong vaporization and bubble formation at the keyhole tip. Miyagi [14] suggested that the bubbles were formed by extra evaporation of the weld metal at the keyhole bottom because of the slight heat input variation. The bubble formation in laser butt welding of aluminum was also studied based on the X-ray phase contrast method [15]. However, the high speed X-ray system is very expensive. Besides, the resolution is low, so some important behavior, such as small bubble formation, can't be observed.

The numerical simulation is also an effective method to get the mechanism of keyhole-induced bubble formation in laser welding. The X-ray system was used, and a semi-analytical mathematic model was developed by Kaplan to study the keyhole collapse in laser welding of liquid zinc [16]. The bottleneck keyhole shape was found to be easily collapsed. Cho [17] used the adiabatic bubble model to model the bubble formation in laser welding. The bubble was assumed to be filled with ideal gas. Heat and mass transfer between the gas and molten metal was ignored. Zhao [18] developed a gas-liquid-solid coupled model to describe the keyhole behavior of laser welding. Keyhole shrinkage and collapse was proposed to be the cause of keyhole-induced bubble and porosity formation. Lu [19] developed a three dimensional transient model to investigate the effect of laser power, welding speed, laser beam size and gap size on keyhole-induced bubble formation in laser welding with T-joint, and suggested that the depth to

* Corresponding author at: Shanghai Key Laboratory of Material Laser Processing and Modification (Shanghai Jiaotong University), Shanghai 200240, PR China.

E-mail address: xmhua@sjtu.edu.cn (X. Hua).

width ratio of the keyhole and fluid flow affected the keyhole-induced bubble formation. Lin [20] suggested that the keyhole collapse between keyhole front and keyhole rear due to the strong melt flow, was the cause of keyhole-induced bubble and porosity formation. It should be noted that only one type of keyhole-induced bubble is analyzed based on simulation.

Berger [21] observed the porosity formation in laser welding of water and ice, and found that the bubbles were generated at the rear side and at the tip of the keyhole. Even though the material properties of water and metals are significant different, several important properties in laser welding are similar. There may be two kinds of keyhole-induced bubble in laser welding.

In this work, laser welding experiment with the aid of glass is carried out, and a three dimensional numerical model considering the shear stress and adiabatic bubble model is developed to study the keyhole behavior and keyhole-induced bubble formation. Two kinds of keyhole-induced bubble are found, and different formation mechanisms responsible for keyhole-induced bubble formation are discussed. The pressure balance equation is proposed to analyze the breaking of molten bridge by the laser beam. The bubble coalescence efficiency is also studied.

2. Experimental procedure

The experimental set-up used for the experiments was shown in Fig. 1. The experiments were performed using a fiber laser welding machine (IPG YLS-10,000), and the focus radius was 0.36 mm. The materials used were Q345 steel with size 100 mm (length) \times 30 mm (width) \times 10 mm (height), and heat resistant quartz glass with size 100 mm (length) \times 10 mm (width) \times 10 mm (height).

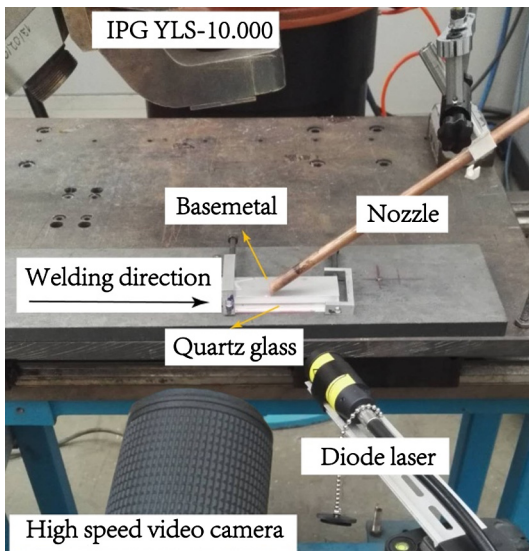


Fig. 1. The experimental platform.

The thermo-physical material properties of Q345 steel can be seen in Table 1. During the welding, the laser beam was tilted in the forward direction with an angle of 10°. The laser power was 6 kW. The defocused distance was 0 mm. The welding speed was 2 m/min. Pure argon gas was used as shielding gas with flow rate of 20 L/min. A high speed video camera was used to observe the keyhole behavior and bubble formation, and the frequency was 3000 frame/s.

3. Mathematical model and numerical simulation

Four governing equations including mass, momentum, energy conservation equations, and VOF (Volume of Fluid) equation are solved to calculate heat and mass transfer in laser welding weld pool. The energy-temperature relationship is used to model the solid-liquid phase change [22] and the porous media drag concept is used to model the flow in the mushy zone [23]. The main driven forces of the weld pool are recoil pressure, shear stress, surface tension force and buoyancy force. The governing equations, recoil pressure, surface tension force, buoyancy force and boundary conditions are same to our previous work [24]. The special treatments on shear stress and adiabatic bubble model are discussed.

3.1. Shear stress model

The flow of the metallic vapor inside the keyhole plays an important role in the keyhole behavior during laser welding [4,25]. It is suggested that the vapor flow is laminar, so the shear stress caused by vapor flow can be expressed as follow [17]:

$$\tau_w = \frac{8\rho V^2}{Re} \quad (1)$$

where V is the vapor velocity, with an assumption that it increases linearly along the keyhole depth. The vapor velocity is zero at the keyhole bottom, while it reaches the maximum value at the entrance of the keyhole.

If the keyhole has a circular tube shape, as shown in Fig. 2(A), Eq. (1) can be used without modification. It should be noted that in laser welding, the shape of the keyhole is in dynamically changing, as shown in Fig. 2(B). So the main problem is how to determine the direction of shear stress. In this study, the value of shear stress is calculated by Eq. (1). It is assumed that the horizontal vector \vec{o} , shear stress vector $\vec{\tau}$, and free surface normal vector \vec{n} are coplanar, as shown in Fig. 2(C). The shear stress vector can be determined as:

$$\begin{cases} \vec{\tau} \cdot \vec{n} = 0 \\ |\vec{\tau}| = \tau_w \\ \vec{\tau} = A\vec{o} + B\vec{n} \end{cases} \quad (2)$$

3.2. Adiabatic bubble model

The adiabatic bubble model is introduced to model the bubble formation. It is assumed that there is no heat transfer and mass

Table 1
Thermo-physical material properties of Q345 steel.

Nomenclature	Value	Nomenclature	Value
Density (kg/m ³)	7830	Liquidus temperature (K)	1725
Viscosity (kg/m·s)	0.0059	Solidus temperature	1688
Specific heat (l) (J/kg·K)	690	Boiling temperature (K)	3133
Specific heat (s) (J/kg·K)	670	Heat transfer coefficient (W/m ² ·K ⁴)	20
Latent heat of fusion (J/kg)	2.77 \times 10 ⁵	Coefficient of thermal expansion (K ⁻¹)	1.5 \times 10 ⁻⁴
Thermal conductivity (l) (W/m·K)	24.9	Surface tension (N/m)	1.2
Thermal conductivity (s) (W/m·K)	25.7	Surface tension gradient (N/m·K)	-0.0003

Download English Version:

<https://daneshyari.com/en/article/7053733>

Download Persian Version:

<https://daneshyari.com/article/7053733>

[Daneshyari.com](https://daneshyari.com)